THE JOURNAL OF BIOLOGICAL CHEMISTRY VOL. 288, NO. 48, pp. 34612–34626, November 29, 2013

Heme Oxygenase-1 Exerts a Protective Role in Ovalbumin-induced Neutrophilic Airway Inflammation by Inhibiting Th17 Cell-mediated Immune Response*

Received for publication, June 20, 2013, and in revised form, October 3, 2013 Published, JBC Papers in Press, October 4, 2013, DOI 10.1074/jbc.M113.494369

Yanjie Zhang[1], **Liya Zhang**[1], **Jinhong Wu, Caixia Di, and Zhenwei Xia**[2]

From the Department of Pediatrics, Ruijin Hospital Affiliated with Shanghai Jiao Tong University School of Medicine, Shanghai 200025, China

Background: Heme oxygenase-1 (HO-1) is an inducible enzyme that exerts multiple physiological functions.
Results: Induction of HO-1 inhibits Th17-mediated neutrophilic airway inflammation *in vivo* and suppresses Th17 cell differentiation *in vitro*.
Conclusion: HO-1 exhibits anti-inflammatory activity in non-eosinophilic asthma (NEA) by inhibiting Th17 responses.
Significance: HO-1 may become a novel therapeutic target in NEA.

Allergic asthma is conventionally considered as a Th2 immune response characterized by eosinophilic inflammation. Recent investigations revealed that Th17 cells play an important role in the pathogenesis of non-eosinophilic asthma (NEA), resulting in steroid-resistant neutrophilic airway inflammation. Heme oxygenase-1 (HO-1) has anti-inflammation, anti-oxidation, and anti-apoptosis functions. However, its role in NEA is still unclear. Here, we explore the role of HO-1 in a mouse model of NEA. HO-1 inducer hemin or HO-1 inhibitor tin protoporphyrin IX was injected intraperitoneally into ovalbumin-challenged DO11.10 mice. Small interfering RNA (siRNA) was delivered into mice to knock down HO-1 expression. The results show that induction of HO-1 by hemin attenuated airway inflammation and decreased neutrophil infiltration in bronchial alveolar lavage fluid and was accompanied by a lower proportion of Th17 cells in mediastinal lymph nodes and spleen. More importantly, induction of HO-1 down-regulated Th17-related transcription factor retinoic acid-related orphan receptor γt (RORγt) expression and decreased IL-17A levels, all of which correlated with a decrease in phosphorylated STAT3 (p-STAT3) level and inhibition of Th17 cell differentiation. Consistently, the above events could be reversed by tin protoporphyrin IX. Also, HO-1 siRNA transfection abolished the effect of hemin induced HO-1 *in vivo*. Meanwhile, the hemin treatment promoted the level of Foxp3 expression and enhanced the proportion of regulatory T cells (Tregs). Collectively, our findings indicate that HO-1 exhibits anti-inflammatory activity in the mouse model of NEA via inhibition of the p-STAT3-RORγt pathway, regulating kinetics of RORγt and Foxp3 expression, thus providing a possible novel therapeutic target in asthmatic patients.

Asthma is a common chronic inflammatory disease, the incidence of which is gradually increasing worldwide due to factors such as environmental pollution. It is of particular concern that severe asthma comprises an important source of morbidity in asthmatic patients and brings a tremendous economic burden to society. Classically, eosinophilic inflammation mediated by Th2 cells is considered a hallmark of asthma. However, recent studies using sputum induction and bronchial alveolar lavage (BAL)[3] techniques indicate that ~50% of asthma is based on non-eosinophilic inflammation-involved polymorphonuclear neutrophils, mast cells, leukomonocytes, and macrophages (1–3). These findings suggest that severe asthma may be a different subtype, namely non-eosinophilic asthma (NEA), rather than just an increase in asthma symptoms *per se* (4). Different from patients with eosinophilic asthma, patients with NEA exhibit non-Th2-type airway inflammation characterized by increased neutrophil levels without elevation of serum IgE (5). Studies indicate that Th17 cells play a crucial role in neutrophilic inflammation, as they secrete IL-17 to induce granulopoiesis, neutrophil chemotaxis, and the anti-apoptotic properties of granulocyte-colony stimulating factor (6). Clinical evidence has also shown that gene expression of IL-17 is elevated in asthmatic patients, a circumstance that is correlated with clinical severity (7). Notably, Th17 cell-mediated airway inflammation and airway hyper-responsiveness are steroid-resistant (8). Therefore, it is imperative to explore novel therapeutic strategies for NEA.

Heme oxygenase (HO) is a rate-limiting enzyme for heme metabolism that catalyzes heme into carbon monoxide (CO), biliverdin, and free iron. Three HO isozymes have been identified, including inducible HO-1, constitutive HO-2, and isomer HO-3. HO-1 is a ubiquitous stress-inducible protein with broad physiological anti-apoptotic, anti-proliferation, and immunoregulatory functions (9–12). As a substrate of HO-1, hemin is

* This work was supported by National Natural Science Foundation of China Grants 81070022, 81128001, and 81270084 and Shanghai Municipal Science and Technology Commission Foundation Grants 13XD1402800 and 10410701000.

[1] Both authors contributed equally to this work.

[2] To whom correspondence should be addressed: Dept. of Pediatrics, Ruijin Hospital, Ruijin 2nd Rd. 197, Shanghai 200025, China. E-mail: xzw63@hotmail.com.

[3] The abbreviations used are: BAL, bronchial alveolar lavage; HO-1, heme oxygenase-1; SnPP, tin-protoporphyrin; OVA, ovalbumin; BALF, bronchial alveolar lavage fluid; NEA, non-eosinophilic asthma; MLN, mediastinal lymph node; FCM, flow cytometry; FAM, carboxyfluorescein; RORγt, retinoic acid-related orphan receptor γt.

widely used to induce HO-1, exerting a protective effect in a variety of animal models (13–15). It is reported that the expression of HO-1 protein and its activity are significantly increased after hemin treatment, whereas the competitive inhibitor tin protoporphyrin IX (SnPP) induces the expression of HO-1 accompanied by blocked enzymatic activity in both animal models and cultured cells (16–21). Our previous studies indicate that induction of HO-1 by hemin is able to suppress allergic airway inflammation in a mouse model of eosinophilic asthma (16). The current study sets out to examine the effect of HO-1 induction on Th17-mediated neutrophilic airway inflammation in DO11.10 T-cell receptor transgenic mice and investigate the mechanism by which HO-1 regulates Th17 immunity.

EXPERIMENTAL PROCEDURES

Mice—DO11.10 T-cell receptor transgenic mice on a BALB/c background were purchased from Model Animal Research Center of Nanjing University and maintained in specific pathogen-free conditions in the Research Center for Experimental Medicine of Ruijin Hospital affiliated with Shanghai Jiao Tong University School of Medicine. All animal experiments were approved by and performed in compliance with the guidelines of the Ethics Committee of Ruijin Hospital affiliated with Shanghai Jiao Tong University School of Medicine.

Induction of the Non-eosinophilic Asthma Model and Administration of Hemin or SnPP—6–8-Week-old female DO11.10 transgenic mice were randomly divided into four groups including OVA, OVA + hemin, OVA + SnPP, and control groups ($n = 6$ in each group). The mice in OVA, OVA + hemin, and OVA + SnPP groups were intranasally challenged with 100 μg of OVA (Sigma) in 50 μl of normal saline after anesthetization by inhalation of isoflurane on days 0, 1, and 2. The mice in the control group were intranasally challenged with normal saline. All animals were sacrificed on day 3. Mice were intraperitoneally administered 75 μmol/kg hemin (Sigma) or 75 μmol/kg SnPP (Porphyrin Products) on days −2 and −1 in OVA + hemin and OVA + SnPP groups, respectively. Hemin or SnPP was dissolved in 0.2 mol/liter NaOH, titrated to pH 7.4 with 0.2 mol/liter HCl, and then diluted with phosphate-buffered saline (PBS).

Bronchoalveolar Lavage Fluid (BALF)—Twenty-four hours after the final challenge (day 3), all mice were anesthetized with isoflurane and sacrificed after collecting blood via the ophthalmic vein. After blunt dissection of the tracheas, the lungs were lavaged three times with ice-cold saline (0.4 ml each) using a 22-gauge intravenous catheter, and the BALF was collected. This procedure recovered 80–90% of the infused fluid. The collected BALF was centrifuged at 453 × *g* at 4 °C for 5 min. The supernatant was then stored at −80 °C before further study. The cells were resuspended in 0.5 ml PBS, and the total cell numbers were counted with a hemocytometer. A small amount of the cell suspension was fixed in 95% ethanol for 30 min for routine H&E staining. On the basis of the findings with H&E stain, cell differentials were counted with at least 200 leukocytes in each sample under the microscope (Olympus AX70, Japan). The cell types were judged according to standard hemocytologic procedures as macrophages, neutrophils, lymphocytes, or eosinophils.

Histopathology—After perfusion with PBS, the right low pulmonary lobes were resected and fixed with 10% neutral buffered formalin and embedded in paraffin. Four-micrometer-thick sections were stained with H&E.

Real-time PCR—Lung tissue was removed and homogenized, and total RNA was extracted with TRIzol reagent (Invitrogen) according to the manufacturer's instructions. Reverse transcription was performed using PrimeScript reverse transcriptase (TaKaRa) to obtain cDNA samples. Real-time PCR was performed using an ABI Prism 7300 (Applied Biosystems) with the following program: 95 °C for 10 s and 40 cycles of amplification at 95 °C for 5 s, 60 °C for 31 s, and 95 °C for 15 s and finally 60 °C for 30 s and 95 °C for 15 s. Relative levels of target mRNA were compared with β-actin using the $2^{-\Delta\Delta Ct}$ method. All primers were synthesized by Shanghai Shengon Biotech Company (Shanghai, China). Sequences were as follows: β-actin forward 5′-GGC TGT ATT CCC CTC CAT CG-3′, reverse 5′-CCA GTT GGT AAC AAT GCC ATG T-3′; Foxp3 forward 5′-CAC AAT ATG CGA CCC CCT TTC-3′, reverse 5′-AAC ATG CGA GTA AAC CAA TGG TA-3′; retinoic acid-related orphan receptor γt (RORγt) forward 5′-GAC CCA CAC CTC ACA AAT TGA −3′, reverse 5′-AGT AGG CCA CAT TAC ACT GCT-3′; T-bet forward 5′-TTT CCA AGA GAC CCA GTT CAT TG-3′, reverse 5′-ATG CGT ACA TGG ACT CAA AGT T-3′; GATA-binding protein 3 (GATA-3) forward 5′-CTC GGC CAT TCG TAC ATG GAA-3′, reverse 5′-GGA TAC CTC TGC ACC GTA GC-3′.

Western Blot Analysis—Lung tissues were homogenized with ice-cold radioimmune precipitation assay buffer (Beyotime, Shanghai, China) containing protease inhibitors. Whole-cell extracts from $CD4^+$ T cells stimulated with recombinant IL-6 (R&D Systems, Minneapolis, MN) or IL-2 (R&D Systems) were also obtained utilizing ice-cold radioimmune precipitation assay buffer. The extracts containing 30 μg of proteins were separated on 12% SDS-PAGE and then transferred to polyvinylidene fluoride membranes. The membrane was blocked with Tris-buffered saline Tween 20 buffer containing 5% skim milk and incubated with the following primary antibodies: rabbit anti-mouse RORγt IgG (1/1000 dilution, Santa Cruz Biotechnology, Santa Cruz, CA), rabbit anti-mouse IgG Foxp3 (1/1000 dilution, Santa Cruz Biotechnology), mouse anti-mouse phosphorylated STAT3 (p-STAT3) (Tyr-705) (1/1000 dilution, Cell Signaling), and mouse anti-mouse phosphor-Stat5 (Tyr-694) (1/1000 dilution, Cell Signaling). The samples were incubated overnight followed by the addition of their corresponding horseradish peroxidase-conjugated anti-rabbit or anti-mouse IgG secondary antibodies (1/5000 dilution, Cell Signaling). The signals were visualized via enhanced chemiluminescence using a Thermo ECL kit (Thermo Fisher Scientific, Waltham, MA) in accordance with the manufacturer's instructions.

ELISA—The concentrations of interferon (IFN)-γ, IL-4, IL-17A (Biolegend, San Diego, CA), and IL-10 (R&D Systems) in BALF or cell culture supernatant were analyzed with ELISA kits in accordance with the manufacturers' instructions.

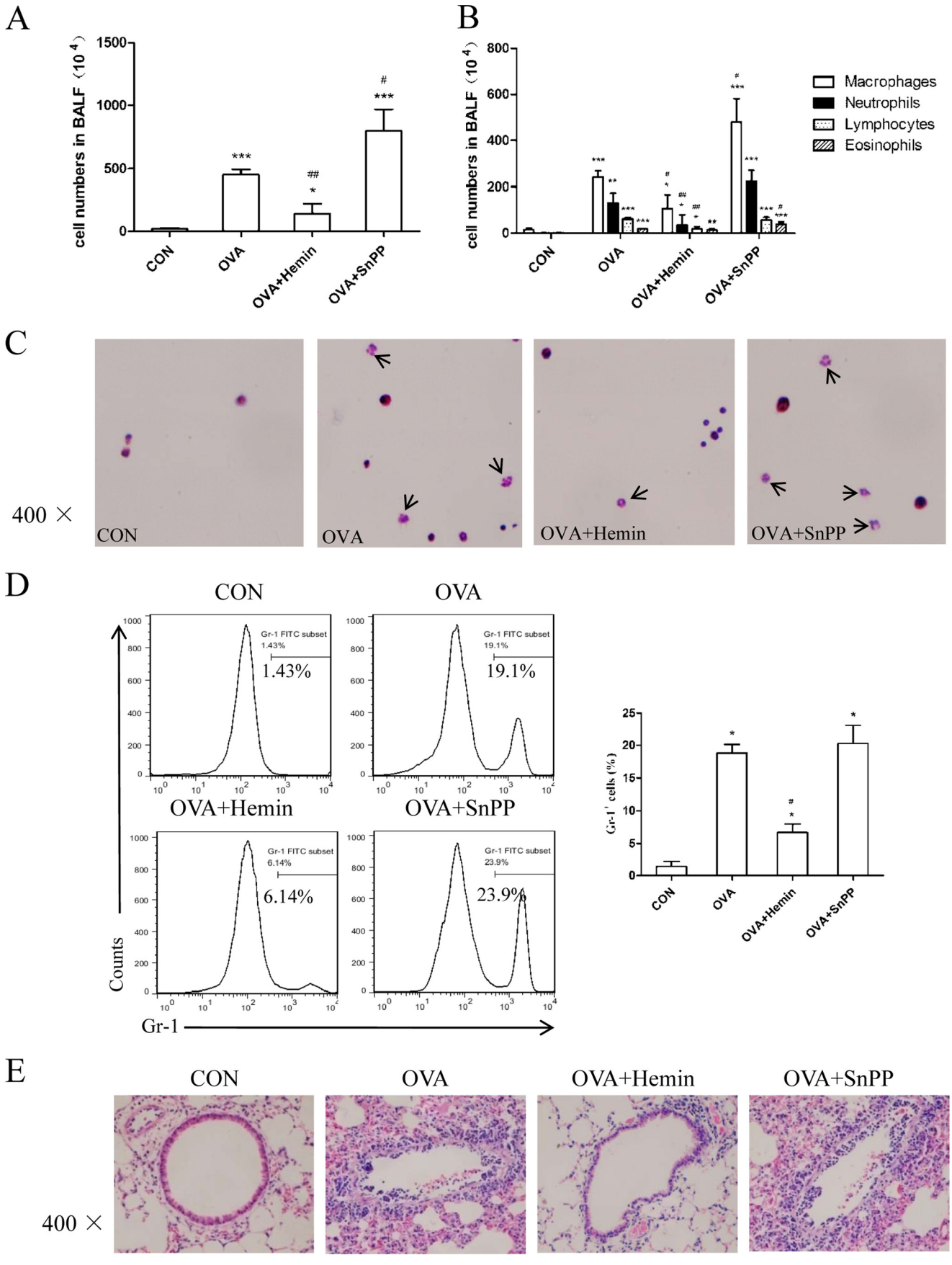
A
cell numbers in BALF (10^4)
1500
1000
500
0
CON
OVA
OVA+Hemin
OVA+SnPP
B
cell numbers in BALF (10^4)
800
600
400
200
0
Macrophages
Neutrophils
Lymphocytes
Eosinophils
C
400 ×
CON
OVA
OVA+Hemin
OVA+SnPP
D
CON
OVA
Gr-1 FITC subset
1.43%
19.1%
OVA+Hemin
OVA+SnPP
6.14%
23.9%
Counts
Gr-1
Gr-1+ cells (%)
E
CON
OVA
OVA+Hemin
OVA+SnPP
400 ×

Flow Cytometry—BALF cells were labeled with FITC anti-Ly-6G (Gr-1) mAb (eBioscience) for 40 min. Mediastinal lymph nodes (MLNs), and spleens were isolated. The cell clumps were disaggregated into single-cell suspensions using nylon mesh (70-μm pore size) filtration. Erythrocytes were lysed with hypotonic buffer (0.15 mol/liter NH_4Cl, 10 mmol/liter $KHCO_3$, 0.1 mmol/liter Na_2EDTA). For detection of Th1, Th2, Th17, and Treg cells, cells were stimulated with lymphocyte activator mixture (phorbol 12-myristate 13-acetate/ionomycin/brefeldin A, BD Pharmingen) for 5 h and labeled with surface markers FITC anti-CD4 mAb (eBioscience) or allophycocyanin anti-CD25 mAb (eBioscience). After washing, fixing, and permeabilizing according to the manufacturer's instructions (eBioscience), cells were labeled intracellularly with allophycocyanin anti-IFN-γ mAb (eBioscience), phosphatidylethanolamine (PE) anti-IL-4 mAb (eBioscience), PE-Cy7 anti-IL-17 mAb (Biolegend), or PE anti-Foxp3 mAb (eBioscience). All labeled cells were detected using flow cytometry (FCM) on the FACScan Flow Analyzer. The data were analyzed with FlowJo 7.6v software.

HO-1 Activity Assay—HO-1 enzyme activity was quantified by measuring bilirubin production (16). Briefly, lung tissues were homogenized on ice in 1 volume of 100 mmol/liter phosphate buffer containing 2 mmol/liter $MgCl_2$ and centrifuged at 18,000 $\times$ *g* for 15 min at 4 °C. The supernatant was used to measure HO activity. The reaction mixture, consisting of 200 μl of sample homogenate, 100 μl of normal liver cytosol (source of biliverdin reductase), 20 μmol/liter hemin, and 0.8 mmol/liter NADPH was incubated at 37 °C for 1 h. The optical density was measured between 464 and 530 nm (extinction coefficient, 40 mmol/liter/cm for bilirubin) to assess bilirubin production once the reaction was terminated. Values were expressed as pmol of bilirubin formed/1 h/mg of protein. An NADPH-free reaction mixture provided a base line against which the measured concentrations were determined.

HO-1 Small-interfering RNA (siRNA) Treatment in Vivo—The carboxyfluorescein (FAM)-labeled HO-1 siRNA (sense 5′-GCU GAC AGA GGA ACA CAA ATT-3′; antisense 5′-UUU GUG UUC CUC UGU CAG CTT-3′) against mouse HO-1 mRNA and scrambled siRNA were synthesized and purchased from Shanghai GenePharma Co., Ltd. 6–8-Week-old female DO11.10 mice (n = 6) were injected via tail vein with 5 optical density/20 g of body weight HO-1 siRNA or scrambled siRNA on day −3. EntransterTM-in vivo transfection reagent (Engreen Biosystem) was used to deliver the siRNA according to the manufacturer's recommendations. Then mice were intraperitoneally administered 75 μmol/kg hemin on days −2 and −1 followed by intranasal challenge with 100 μg of OVA in 50 μl of normal saline after anesthetization by inhalation of isoflurane on days 0, 1, and 2. Mice were sacrificed 24 h after the transfection (day −2) and the final challenge (day 3). Lung tissues were immediately removed and frozen in liquid nitrogen. The tissues were embedded in optimum cutting temperature (OCT) compound (Sakura), and sections (7 μm) were cut from the blocks followed by fixed in cold acetone for 30 min. Slides were stained with 4′,6-diamidino-2-phenylindole (DAPI) and washed with PBS three times. A fluorescence microscopy (Nikon Ti-S) was used for data acquisition.

Th17 Cell Differentiation in Vitro—Naive $CD4^+$ T cells were purified from BALB/c mouse spleens via magnetic isolation (MiltenyiBiotec, Bergisch Gladbach, Germany). For the preparation of spleen cell suspensions, spleens from 8-week-old female BALB/c mice were removed and minced with a nylon mesh (70-μm pore size). After the cells were pelleted, erythrocytes were lysed with hypotonic buffer. Naive $CD4^+$ T cells were purified according to the manufacturer's instructions and then marked with carboxyfluorescein succinimidyl ester (Invitrogen). Cells were seeded at a density of 1×10^6/well in 48-well plates and cultured in RPMI 1640 medium (HyClone) supplemented with 1% L-glutamine (0.2 mol/liter), 10% fetal calf serum, 100 IU/ml penicillin/streptomycin, 1% HEPES (1 mol/liter), 1% sodium hydrogen carbonate (100 mmol/liter), and 0.1% 2-β-mercaptoethanol (50 mmol/liter, Invitrogen). The cells were activated with plate-bound anti-CD3 (2 μg/ml) and soluble anti-CD28 (2 μg/ml) antibodies (eBioscience). T helper (Th)-neutral conditions (Th0) included no exogenous cytokines or anti-cytokines. For Th17 differentiation, cells were stimulated with TGF-β1 (5 ng/ml, Cell Signaling), IL-6 (50 ng/ml, R&D Systems), IL-23 (20 ng/ml, R&D Systems), anti-IFN-γ (10 μg/ml, Biolegend), and anti-IL-4 (10 μg/ml, Biolegend). Hemin and SnPP were dissolved in 0.2 mol/liter NaOH at a concentration of 50 μmol/ml and added to cultures at an appropriate concentration of 30 nmol/ml.

STAT Phosphorylation Assays—DO11.10 mice were intraperitoneally injected with or without 75 μmol/kg hemin or 75 μmol/kg SnPP for 2 days (one time a day) to induce HO-1 with or without enzymatic activity. Because we determined that the maximal induction of HO-1 protein and its activity occurred at 24 h after hemin treatment, accompanied with the lowest enzymatic activity at the same time after SnPP treatment in a previous study (16), mice were sacrificed here to isolate spleens 24 h after the second hemin/SnPP injection. The cell clumps were disaggregated into single-cell suspensions using nylon mesh (70 μm pore size) filtration followed by lysis of erythrocytes with hypotonic buffer. $CD4^+$ T cells were purified using a $CD4^+$ T Cell Isolation Kit II (MiltenyiBiotec) according to the manufacturer's instructions. Purified $CD4^+$ T cells from normal, hemin-treated, and SnPP treated mice were cultured in medium supplemented with recombinant IL-6 (50 ng/ml, R&D System) or IL-2 (200 units/ml, R&D System) for

FIGURE 1. **HO-1 alleviates OVA-induced neutrophilic airway inflammation in DO11.10 mice.** *A*, the total cell counts in BALF (* compared with the control (CON) group: *, $p < 0.05$; ***, $p < 0.001$; # with the OVA group: #, $p < 0.05$; ##, $p < 0.01$). *B*, the differential cell counts identified by morphologic criteria in BALF (* compared with the control group: *, $p < 0.05$; **, $p < 0.01$; ***, $p < 0.001$; # with the OVA group: #, $p < 0.05$; ##, $p < 0.01$). *C*, cytospin preparations of BALF cells from four groups stained with hematoxylin and eosin (original magnification ×400). *Arrows* indicate neutrophils with lobed nucleus in BALF. *D*, flow cytometric analysis of BALF cells from four groups. *Numbers in the graph* indicate the percentages of neutrophils ($Gr\text{-}1^+$) (* compared with the control group: *$p < 0.05$; # with OVA group, ##$p < 0.01$). *E*, histological analysis of lung tissues isolated from DO11.10 mice in control, OVA, OVA + hemin, and OVA + SnPP groups. Paraffin-embedded lung sections were prepared 24 h after the last OVA challenge and were stained with hematoxylin and eosin to observe inflammation (original magnification ×400). Each symbol in the graph represents an individual mouse ($n = 6$). All results shown are representative of three independent experiments.

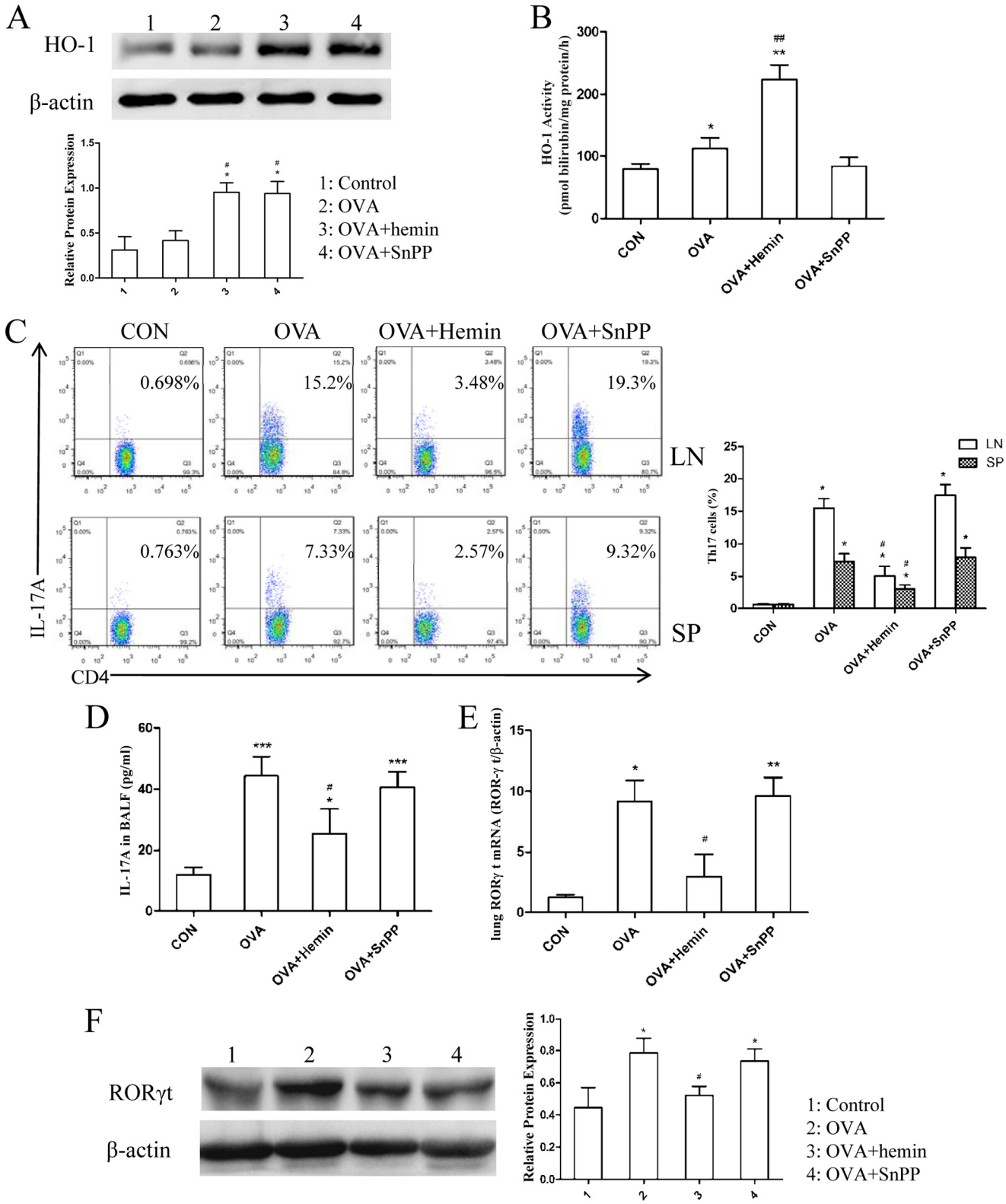

FIGURE 2. **Induction of HO-1 suppresses Th17-mediated response in DO11.10 mice.** *A*, Western blot analysis of HO-1 protein expression in lung tissues extracted from four groups. β-Actin was used as the loading control. Densitometry analysis was performed by normalizing to β-actin levels (* compared with the control group: *, $p < 0.05$; # with compared with the OVA group: #, $p < 0.05$). *B*, the analysis of HO-1 activity in lung tissues extracted from four groups (* compared with the control (*CON*) group: *, $p < 0.05$; **, $p < 0.01$; # compared with the OVA group; ##, $p < 0.01$). *C*, flow cytometric analysis of mediastinal lymph node (*LN*) and spleen (*SP*) cells isolated from DO11.10 mice in control, OVA, OVA + hemin, and OVA + SnPP groups. Numbers in the *upper right quadrants* indicate the percentages of Th17 ($CD4^+IL\text{-}17^+$) cells gated on $CD4^+$ T cells. Each symbol in the graph represents an individual mouse ($n = 6$). *D*, ELISA analysis of IL-17A in BALF from four groups (* compared with the control group: *, $p < 0.05$; ***, $p < 0.001$; # compared with the OVA group: #. $p < 0.05$). *E*, real-time PCR analysis of RORγt mRNA in lung tissues isolated from four groups (* compared with the control group: *, $p < 0.05$; **, $p < 0.01$; # compared with the OVA group, #$p < 0.05$). *F*, Western blot analysis of RORγt protein expression in lung tissues extracted from four groups. β-Actin was used as the loading control. Densitometry analysis was performed by normalizing to β-actin levels (* compared with the control group: *, $p < 0.05$; #, compared with the OVA group: #, $p < 0.05$). All results shown are representative of three independent experiments.

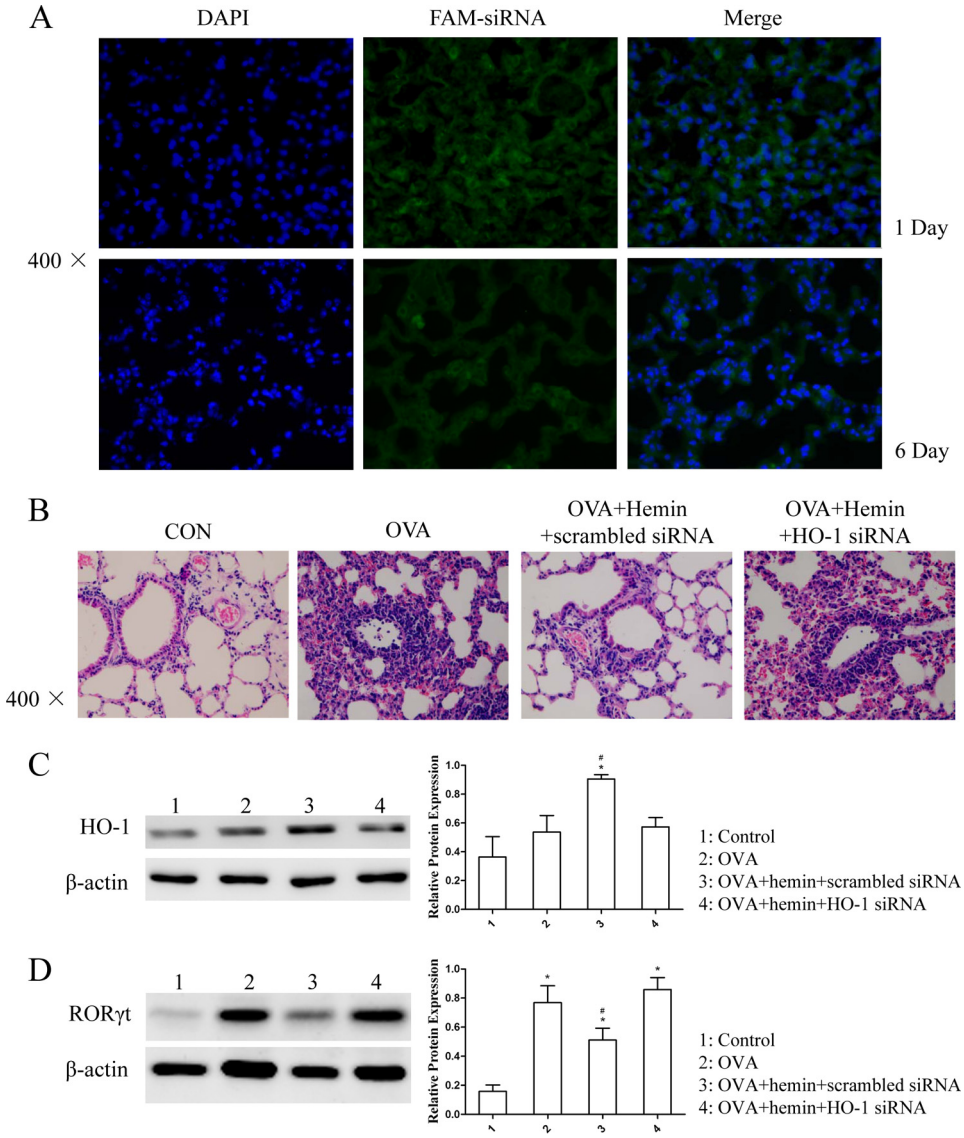

FIGURE 3. **Silencing of HO-1 with siRNA abolished the effect of HO-1 induction *in vivo*.** *A*, the distribution of FAM-siRNA in lung tissues isolated from DO11.10 mice. OCT-embedded lung sections were prepared 24 h after transfection (day −2) and 1 day after the last OVA challenge (6 days after the transfection (day 3)) and stained with DAPI. The FAM-expressing cells in lung tissues were visualized under a fluorescence microscope (original magnification ×400). *B*, histological analysis of lung tissues isolated from DO11.10 mice in control (*CON*), OVA, OVA + hemin + scrambled siRNA, and OVA + hemin + HO-1 siRNA groups. Paraffin-embedded lung sections were prepared 1 day after the transfection (day −2) and 1 day after the last OVA challenge (6 days after the transfection (day 3)) and stained with hematoxylin and eosin to observe inflammation (original magnification ×400). Each symbol in the graph represents an individual mouse ($n = 6$). *C*, Western blot analysis of HO-1 protein expression in lung tissues was extracted from the four groups. β-Actin was used as the loading control. Densitometry analysis was performed by normalizing to β-actin levels (* compared with the control (*CON*) group: *, $p < 0.05$; #, compared with the OVA group: #, $p < 0.05$). *D*, Western blot analysis of RORγt protein expression in lung tissues extracted from the four groups. β-Actin was used as the loading control. Densitometry analysis was performed by normalizing to β-actin levels (* compared with the control group: *, $p < 0.05$; # compared with the OVA group: #, $p < 0.05$). All results shown are representative of three independent experiments.

1 h to phosphorylate transcription factors STAT3 or STAT5, respectively. Cell lysate was assessed for the expression of p-STAT3 or p-STAT5 by Western blot analysis.

Statistical Analysis—Data are presented as the mean ± S.D. The differences between mean values were calculated using an unpaired *t* test or nonparametric statistics. $p < 0.05$ was considered statistically significant.

RESULTS

HO-1 Alleviates OVA-induced Neutrophilic Airway Inflammation in DO11.10 Mice—Previously, we found that up-regulation of HO-1 could protect against OVA-sensitized/challenged eosinophilic airway inflammation (16). Thus, we investigated the effect of HO-1 on neutrophilic airway inflammation in DO11.10 mice. The mice are transgenic for T-cell receptor specific for MHC-II-restricted OVA peptide and are known to develop a neutrophilic lung inflammation upon exposure to OVA aerosols without any sensitization dependent on Th17 cells (22–24). Mice were challenged with OVA or normal saline, and hemin and SnPP, respectively, were injected intraperitoneally 2 days before OVA inhalation. Twenty-four hours after the last challenge, mice were subjected to BAL for airway inflammation analysis. Compared with the control group, the OVA group had a significantly higher total num-

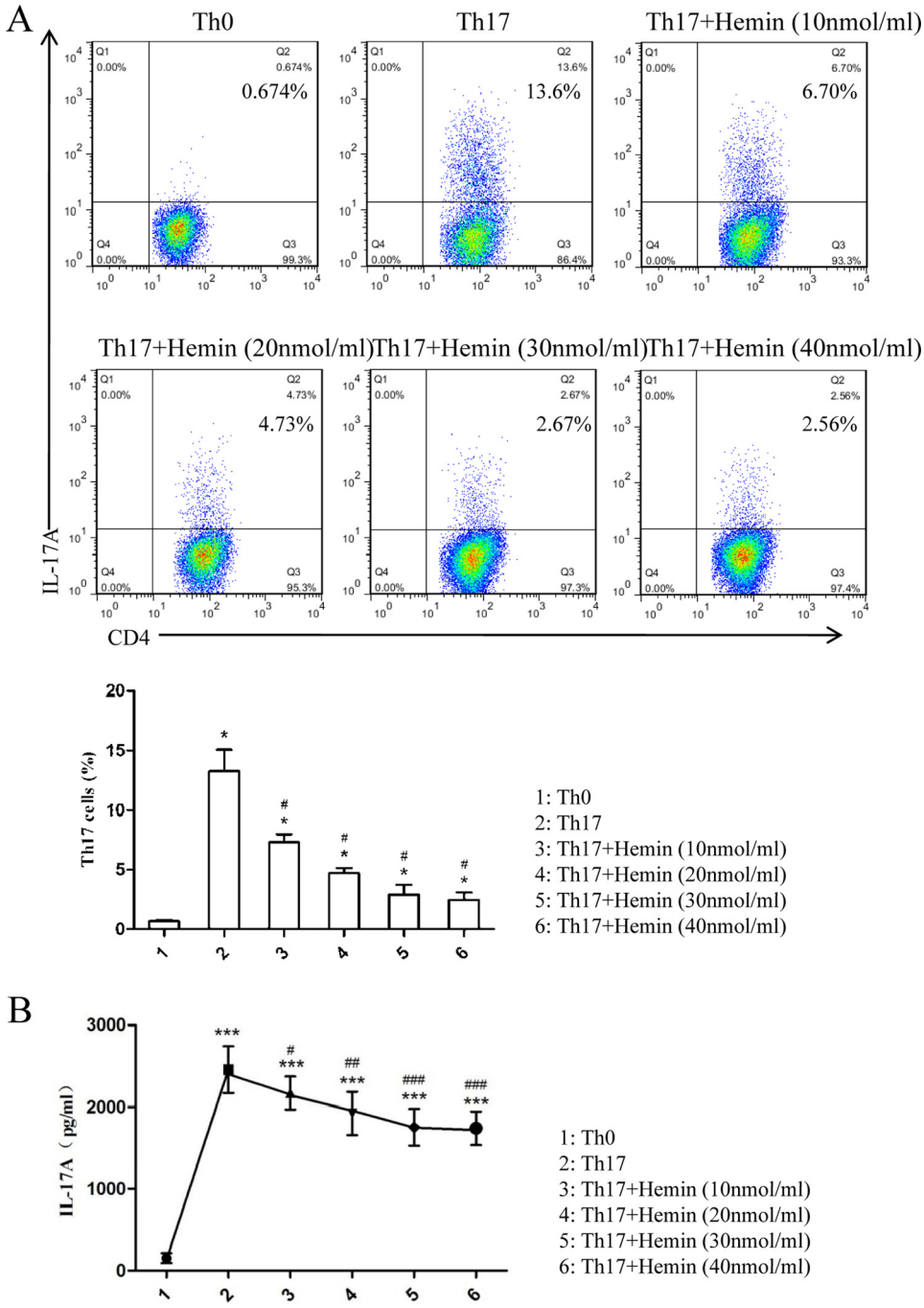

FIGURE 4. **Hemin inhibits Th17 cell differentiation in a dose-dependent manner *in vitro*.** *A*, flow cytometric analysis of magnetically purified naïve T cells from spleens of BALB/c mice cultured under Th17-skewing conditions with or without different concentrations of hemin (10, 20, 30, 40 nmol/ml) for 3 days. *Numbers in the upper right quadrants* indicate the percentages of Th17 ($CD4^+$ $IL\text{-}17^+$) cells gated on $CD4^+$ T cells (* compared with the control group: *, $p < 0.05$; #, with OVA group; #, $p < 0.05$). *B*, ELISA analysis of IL-17A in supernatants of cultured naïve T cells (* compared with the Th0 condition: *. $p < 0.05$; **, $p < 0.01$; ***, $p < 0.001$; # with the Th17-skewing condition: #, $p < 0.05$, ##, $p < 0.01$; ###, $p < 0.001$). All results shown are representative of three independent experiments.

ber of cells in BALF (Fig. 1*A*). Further assessment of cell morphology indicated that the OVA group showed an increase in macrophage, neutrophil, lymphocyte, and eosinophil counts (Fig. 1, *B* and *C*). Pretreatment with hemin markedly reduced the total number of cells, especially the number of neutrophils and lymphocytes, whereas SnPP intervention increased the number of these inflammatory cells (Fig. 1, *A*–*C*). To confirm the change of neutrophils in BALF, we analyzed the expression of Gr-1 (a marker on peripheral neutrophils) on BALF cells. As shown in Fig. 1*D*, mice in the OVA group exhibited an increased proportion of neutrophils ($Gr\text{-}1^+$) as compared with the control group. The proportion of neutrophils decreased in the OVA + hemin group (6.14%) *versus* the OVA group (19.1%) but increased in the OVA + SnPP group (23.9%). Meanwhile, OVA inhalation also led to histological structure changes, including peribronchial and perivascular leukocyte infiltration, edema, and epithelial damage (Fig. 1*E*). In mice treated with hemin, inflammatory cell infiltration was ameliorated with

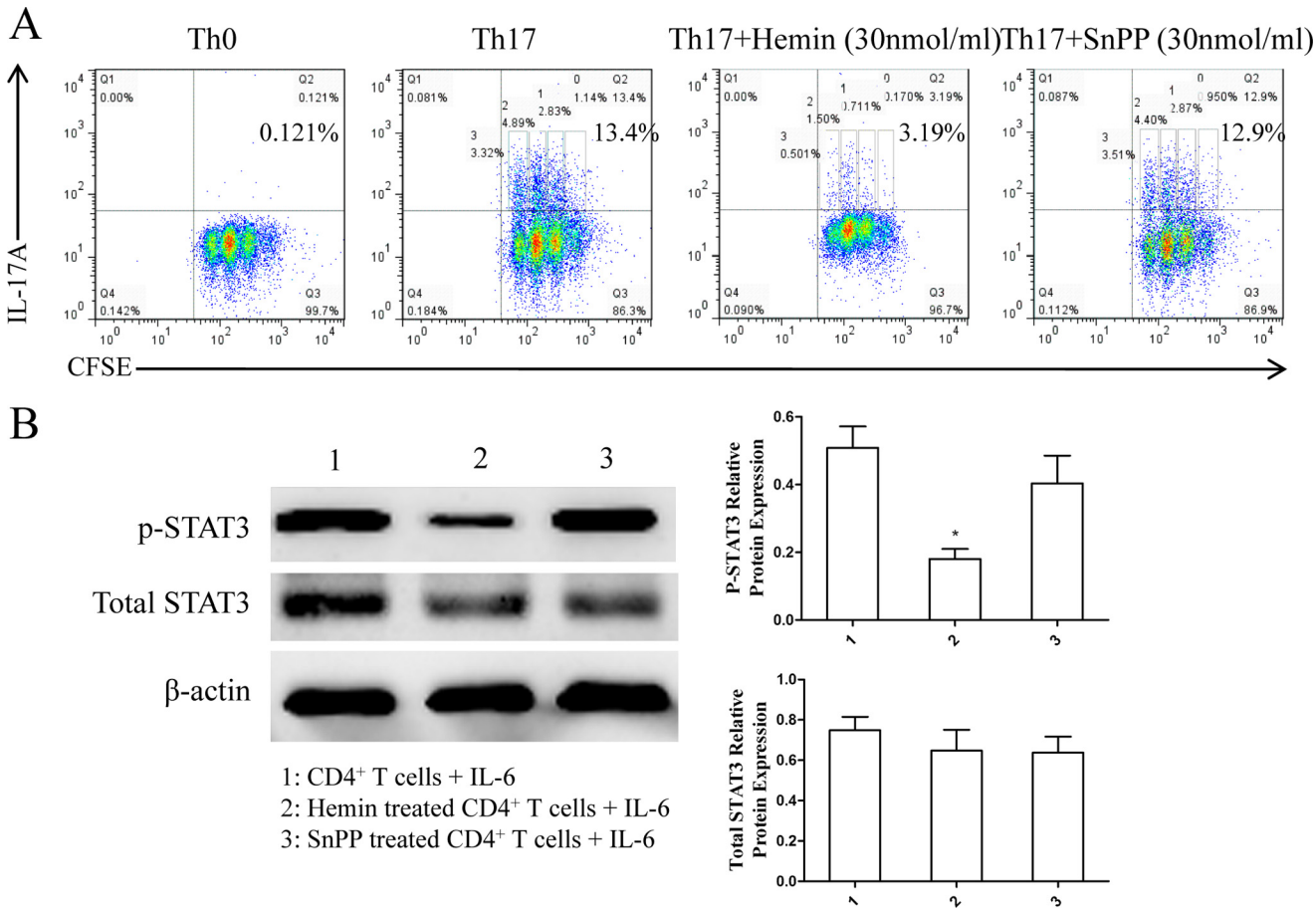

FIGURE 5. **Th17 cell differentiation, $CD4^+$ T cell proliferation, and STAT3 phosphorylation are inhibited by hemin but not by SnPP.** *A*, flow cytometric analysis of magnetically purified naïve T cells from spleens of BALB/c mice cultured under Th17-skewing conditions with or without hemin or SnPP (30 nmol/ml) for 3 days. *Numbers in the upper right quadrants* indicate the percentages of Th17 ($CD4^+IL\text{-}17^+$) cells as well as each generation of Th17 cells (undivided cells (*0*), generation 1 (*1*), generation 2 (*2*), and generation 3 (*3*)) gated on $CD4^+$ T cells. *B*, Western blot analysis of purified $CD4^+$ T cells isolated from DO11.10 mice pretreated with or without hemin and SnPP and cultured with IL-6 for 1 h. *β*-Actin was used as the loading control. Densitometry analysis of p-STAT3 and total STAT3 was performed by normalizing to *β*-actin levels (* compared with $CD4^+$ T cells from untreated mice: *, $p < 0.05$). All results shown are representative of three independent experiments.

much less tissue injury, all of which were exaggerated in the OVA + SnPP group (Fig. 1*E*).

HO-1 Suppresses Th17-mediated Immune Response in Vivo—Next, we evaluated the effect of HO-1 on Th17 response in OVA-induced neutrophilic airway inflammation. Western blot analysis confirmed that the HO-1 protein level in lung tissues was higher in the OVA group than in the control group and significantly increased after administration of hemin accompanied by an enhancement in HO-1 activity (Fig. 2, *A* and *B*). Although pretreatment with SnPP also increased the expression level of HO-1 protein, we observed an unexpected decrease in HO-1 activity (Fig. 2, *A* and *B*). Then MLNs and spleens were harvested to isolate T cells. The proportion of IL-17-producing $CD4^+$ T cells (Th17 cells) was analyzed using FCM. The results showed that the proportions of Th17 cells in MLNs and spleen, enhanced by OVA challenge, were markedly reduced by hemin but reversed by SnPP treatment (Fig. 2*C*). To examine whether induction of HO-1 could inhibit the production of Th17-related cytokine IL-17A, the concentration of IL-17A in BALF was measured using ELISA. As shown in Fig. 2*D*, OVA-challenged mice had a significantly higher concentration of IL-17A as compared with the control group, in which this was reduced in mice pretreated with hemin. There was no significant difference in IL-17A level between the OVA and the OVA + SnPP groups (Fig. 2*D*). In addition, Th17-related transcription factor RORγt mRNA expression in lung tissues was significantly up-regulated in the OVA and the OVA + SnPP groups but declined in the OVA + hemin group (Fig. 2*E*). Meanwhile, we further analyzed the protein levels of RORγt in lung tissues. Consistent with the results described above, the expression of RORγt was also elevated in the OVA and the OVA + SnPP groups but decreased in mice receiving hemin treatment (Fig. 2*F*).

TABLE 1
Proportions of each generation gated on $CD4^+IL\text{-}17A^+$ T cells

Generation	Th0	Th17	Th17 + hemin	Th17 + SnPP
			%	
Undivided cells	0	9.36	5.90	8.10
Generation 1	0	23.23	24.67	24.47
Generation 2	0	40.15	52.05	37.51
Generation 3	0	27.26	17.38	29.92

Silencing of HO-1 with siRNA Abolished the Effect of HO-1 Induction in Vivo—To delineate more precisely the effect of HO-1 in OVA-induced neutrophilic airway inflammation, FAM-labeled siRNA targeting the mouse *HO-1* mRNA was

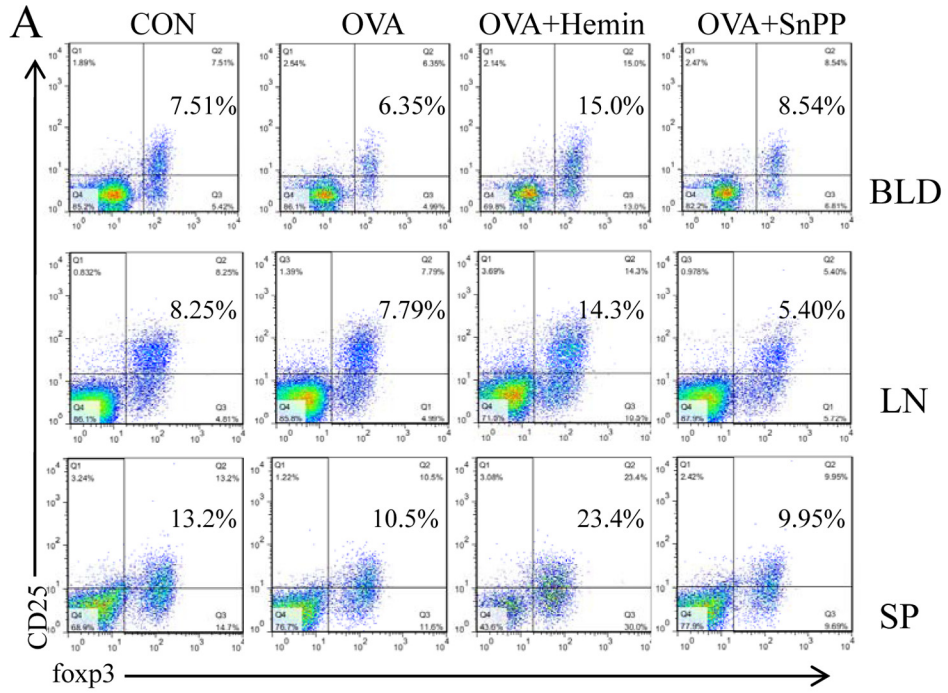
A
CON
OVA
OVA+Hemin
OVA+SnPP
7.51%
6.35%
15.0%
8.54%
BLD
8.25%
7.79%
14.3%
5.40%
LN
13.2%
10.5%
23.4%
9.95%
SP
CD25
foxp3

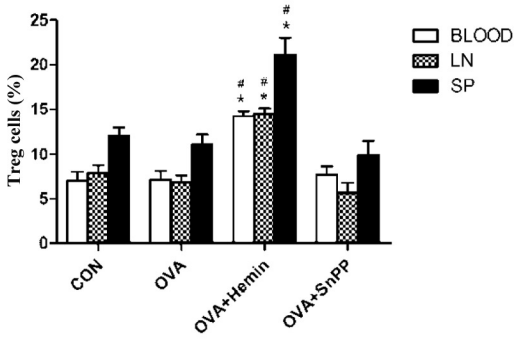
Treg cells (%)
BLOOD
LN
SP
CON
OVA
OVA+Hemin
OVA+SnPP

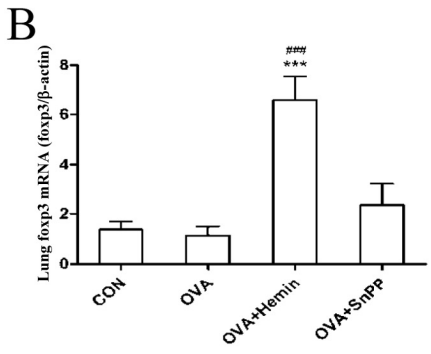
B
Lung foxp3 mRNA (foxp3/β-actin)
CON
OVA
OVA+Hemin
OVA+SnPP

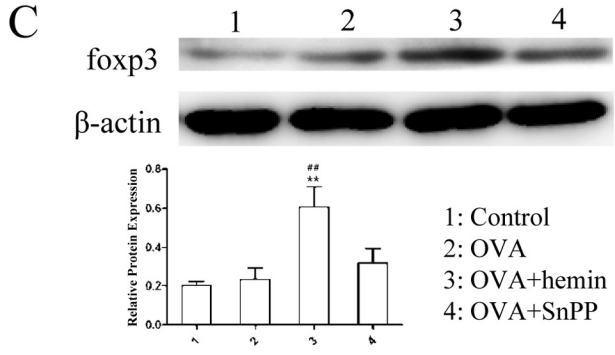
C
1
2
3
4
foxp3
β-actin
Relative Protein Expression
1: Control
2: OVA
3: OVA+hemin
4: OVA+SnPP

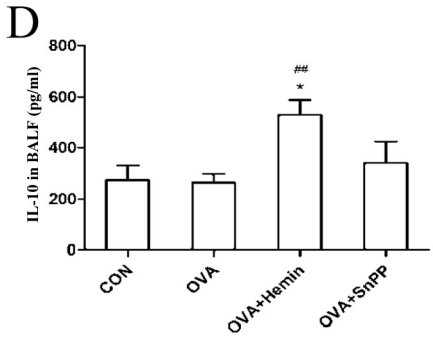
D
IL-10 in BALF (pg/ml)
CON
OVA
OVA+Hemin
OVA+SnPP

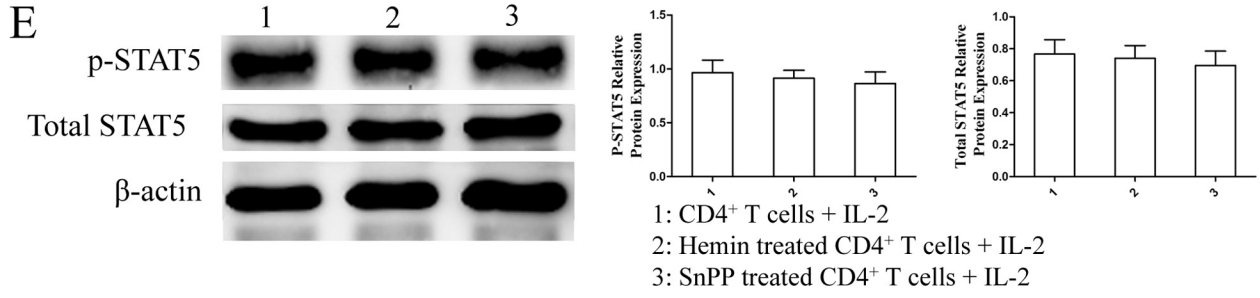
E
1
2
3
p-STAT5
Total STAT5
β-actin
P-STAT5 Relative Protein Expression
Total STAT5 Relative Protein Expression
1: CD4+ T cells + IL-2
2: Hemin treated CD4+ T cells + IL-2
3: SnPP treated CD4+ T cells + IL-2

injected into DO11.10 mice to specifically suppress HO-1 expression. Fluorescence microscopy showed that FAM-expressing cells in lung tissues were visualized 24 h after transfection, and the signals could exist until the end of the experiment (Fig. 3*A*). Furthermore, the results showed that hemin treatment alleviated airway inflammation in mice transfected with scrambled control siRNA, but HO-1 siRNA transfection abolished the anti-inflammatory effect of hemin (Fig. 3*B*). Western blot analysis revealed that HO-1 siRNA transfection significantly reduced the hemin-induced protein level of HO-1 expression in lung tissues, whereas scrambled siRNA did not have this effect (Fig. 3*C*). We also observed that hemin treatment decreased the protein level of RORγt expression in mice transfected with scrambled siRNA, but *HO-1* siRNA transfection nullified the hemin effect (Fig. 3*D*).

Induction of HO-1 Suppresses the Differentiation of Th17 Cells via Inhibition of p-STAT3 in Vitro—Based on the results *in vivo* showing that induction of HO-1 significantly reduced Th17 cell populations, we further evaluated the role of HO-1 in Th17 cell differentiation *in vitro*. Purified naïve $CD4^+$ T cells from BALB/c mouse spleen were cultured under Th17-skewing conditions with or without hemin or SnPP to differentiate into Th17 cells. IL-17A expression was determined by intracellular labeling, and the proportion of IL-17A-producing cells was detected in $CD4^+$ T cells by FCM. The results showed that there was a markedly inhibitory effect of hemin on Th17 cell differentiation occurring in a dose-dependent fashion (Fig. 4*A*). The inhibitory effect of hemin was similar at concentrations of 30 and 40 nmol/ml (Fig. 4*A*). Meanwhile, the levels of IL-17A in supernatants were determined by ELISA analysis. Consistent with the inhibition of Th17 cell differentiation, the levels of IL-17A decreased with increasing concentrations of hemin (Fig. 4*B*). In addition, we observed that Th17 cell differentiation was not affected when 30 nmol/ml SnPP was added to the media, a result opposite to that found with hemin (Fig. 5*A*). Moreover, the proliferation cycles of $CD4^+IL\text{-}17A^+$ T cells in each group appeared as three cycles, with a lower proportion of cells in generation three from hemin (17.38%) as compared with Th0, Th17, and Th17 + SnPP groups (0, 27.26, and 29.92%, respectively) (Table 1). These results suggested that induction of HO-1 enzymatic activity by hemin exerted a mildly inhibitory effect on the proliferation of $CD4^+IL\text{-}17A^+$ T cells but significantly suppressed Th17 cell differentiation.

Because STAT3, a downstream mediator of IL-6R and an important activator of IL-17 and RORγt expression, is necessary for the expression of multiple transcription factors involved in Th17 differentiation and directly regulates the IL-17 gene (25), we supposed that HO-1 could inhibit Th17 differentiation via affecting IL-6-induced phosphorylation of STAT3. Mice were pretreated with hemin or SnPP to elevate the expression of HO-1 in $CD4^+$ T cells, whereas SnPP inhibited the enzymatic activity. After purifying of $CD4^+$ T cells from spleen via magnetic isolation, recombinant IL-6 was added to the culture media to induce phosphorylation of STAT3 in $CD4^+$ T cells. The results show that p-STAT3 level was decreased in $CD4^+$ T cells from mice pretreated with hemin, but the level was only mildly reduced in $CD4^+$ T cells after SnPP treatment with no statistical difference as compared with those from untreated mice. However, the total level of STAT3 expression was not affected by hemin and SnPP treatment (Fig. 5*B*).

HO-1 Up-regulates Treg Cells Independent of Phosphorylated STAT5—The balance between Th17 and Treg cells is crucial for immune homeostasis, as the development of inflammatory disorders may be triggered by an excess in Th17 function or increased numbers of Th17 and defects in Treg function or reduced numbers of Treg (26). Thus, we also investigated the changes in Tregs in this model. $CD4^+CD25^+Foxp3^+$Tregs in peripheral blood, MLNs, and spleen were analyzed using FCM. As expected, the results show that OVA challenge slightly decreased the population of Tregs in DO11.10 mice. There was an increased proportion of $CD4^+CD25^+Foxp3^+$Tregs in the OVA + hemin group *versus* the OVA group, whereas inhibition of HO-1 enzymatic activity by SnPP led to a decline in the population of $CD4^+CD25^+Foxp3^+$Tregs (Fig. 6*A*). Foxp3 mRNA and protein levels in lung tissues were further determined by real-time PCR and Western blot analysis, respectively. The results demonstrate that the levels of Foxp3 mRNA expression and protein were significantly up-regulated by hemin pretreatment (Fig. 6, *B* and *C*). However, this effect of HO-1 was abrogated in the presence of its inhibitor SnPP (Fig. 6, *B* and *C*). In addition, the concentration of anti-inflammatory cytokines IL-10 in BALF was also measured using ELISA. The results show that the levels of IL-10 were markedly elevated by 2-fold in the OVA + hemin group, but no alteration was observed in the OVA + SnPP group (Fig. 6*D*).

It is reported that STAT5, which is activated by IL-2 signaling, has been proved to be a direct transcriptional repressor of the IL-17A gene and critical for Treg cell development and Foxp3 expression (27–29). Therefore, we assessed the effect of HO-1 on STAT5 phosphorylation status to further elucidate the mechanism of HO-1 in regulating Th17/Treg balance. However, the study shows that there were no significant changes in the expression of p-STAT5 or total STAT5 in exogenous IL-2-stimulated $CD4^+$ T cells from mice that received

FIGURE 6. **HO-1 up-regulates Tregs and enhances their functions *in vivo* but has no significant effect on STAT5 phosphorylation.** *A*, flow cytometric analysis of peripheral blood (*BLD*), mediastinal lymph node (*LN*), and spleen (*SP*) cells isolated from DO11.10 mice in control, OVA, OVA + hemin, and OVA + SnPP groups. *Numbers in the upper right quadrants* indicate the percentages of Tregs ($CD4^+CD25^+Foxp3^+$) gated on $CD4^+$ T cells (* compared with control group: *, $p < 0.05$; #, with OVA group; #, $p < 0.05$). Each symbol in the graph represents an individual mouse ($n = 6$). *B*, real-time PCR analysis of Foxp3 mRNA in lung tissues isolated from four groups (* compared with the control (*CON*) group: ***, $p < 0.001$; # compared with the OVA group: ###, $p < 0.001$). *C*, Western blot analysis of Foxp3 protein expression in lung tissues extracted from four groups. β-Actin was used as the loading control. Densitometry analysis was performed by normalizing to β-actin levels (* compared with the control group: **, $p < 0.01$; # compared with the OVA group: ##, $p < 0.01$). *D*, ELISA analysis of IL-10 in BALF collected from four groups (* compared with the control group: *, $p < 0.05$; # compared with the OVA group: ##, $p < 0.01$). *E*, Western blot analysis of purified $CD4^+$ T cells isolated from DO11.10 mice pretreated with or without hemin and SnPP and cultured with IL-2 for 1 h. β-Actin was used as loading control. Densitometry analysis of p-STAT5 and total STAT5 was performed by normalizing to β-actin levels. All results shown are representative of three independent experiments.

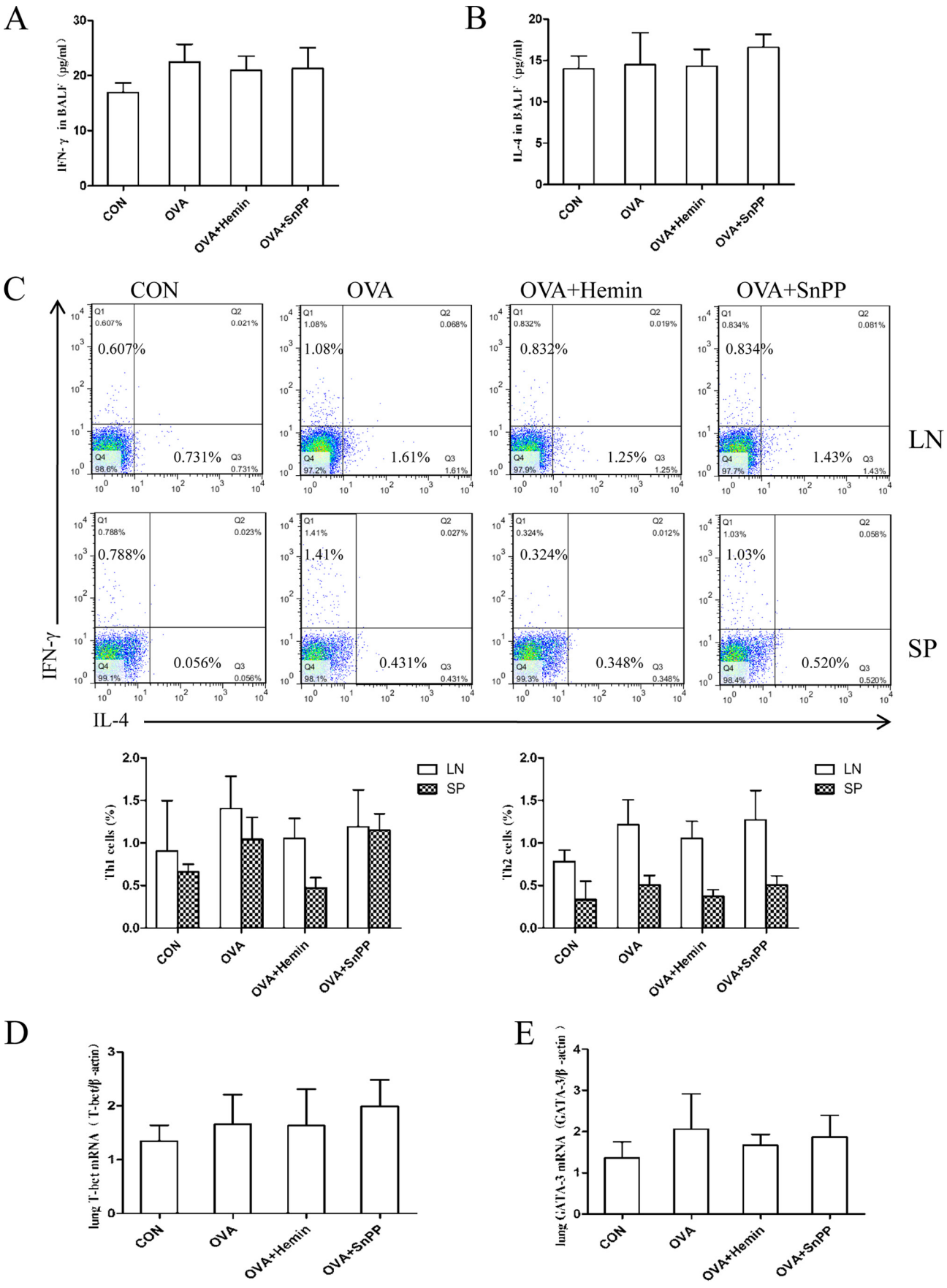
A
IFN-γ in BALF (pg/ml)
CON
OVA
OVA+Hemin
OVA+SnPP
B
IL-4 in BALF (pg/ml)
C
CON
OVA
OVA+Hemin
OVA+SnPP
0.607%
0.731%
1.08%
1.61%
0.832%
1.25%
0.834%
1.43%
LN
0.788%
0.056%
1.41%
0.431%
0.324%
0.348%
1.03%
0.520%
SP
IFN-γ
IL-4
Th1 cells (%)
Th2 cells (%)
D
lung T-bet mRNA (T-bet/β-actin)
E
lung GATA-3 mRNA (GATA-3/β-actin)

hemin or SnPP treatment as compared with untreated mice (Fig. 6*E*). This suggests that induction of HO-1 may not noticeably affect IL-2-induced phosphorylation of STAT5 in $CD4^+$ T cells. The shifted equilibrium between Th17 and Treg cells toward the latter by induction of HO-1 may correlate with its negative action on the phosphorylation of STAT3 in $CD4^+$ T cells.

HO-1 Does Not Noticeably Affect Th1- or Th2-mediated Response in DO11.10 Mice—To observe the effect of HO-1 on other T cell subsets in neutrophilic airway inflammation, we examined Th1/Th2 profiles in the DO11.10 mouse model. The concentrations of Th1-related cytokine IFN-γ and Th2-related cytokine IL-4 in BALF were detected using ELISA. The results indicate that the concentrations of IFN-γ and IL-4 in different groups showed no statistical difference (Fig. 7, *A* and *B*). Additionally, FCM analysis of IFN-γ-producing $CD4^+$ T cells (Th1 cells) and IL-4-producing $CD4^+$ T cells (Th2 cells) indicated that proportions of Th1 and Th2 cells were much lower as compared with that of Th17 cells in OVA-challenged mice (Fig. 7*C*). This study further found that the mRNA levels of Th1 and Th2 lineage-specific transcription factors, T-box transcription factor (T-bet)- and GATA-binding protein 3, fluctuated slightly among different groups, with no statistical significance (Fig. 7, *D* and *E*). These data indicate that airway inflammation induced by OVA challenge results in prominent Th17 responses instead of Th1 or Th2 responses in DO11.10 mice. HO-1 does not noticeably affect Th1 or Th2 response in this model, and its protective effect on neutrophilic airway inflammation is mediated through the suppression of Th17 responses.

DISCUSSION

It has been observed that NEA involves IL-17A to evoke recruitment of neutrophils as one of its hallmarks, in which Th17 cell-mediated neutrophilic airway inflammation is steroid-resistant (8, 30). Therefore, it becomes necessary to identify novel therapeutic targets for developing effective anti-inflammatory medications. To this end we sought to determine whether HO-1 might be proven anti-inflammatory in NEA. In the current study we observe the protective role of HO-1 in OVA-induced neutrophilic airway inflammation in DO11.10 mice. Induction of HO-1 by hemin significantly inhibited Th17 responses through down-regulating Th17-related transcription factors and cytokines, all of which correlated with the suppression of Th17 cell differentiation and the decrease of p-STAT3, so that Th17/Treg balance could be restored. Taken together, these results indicate a possible role of HO-1 as a novel regulator of Th17/Treg balance to alleviate neutrophilic inflammation in NEA.

HO is a rate-limiting microsomal enzyme that catalyzes the degradation of heme to equimolar amounts of ferrous iron, carbon monoxide (CO), and biliverdin, which is rapidly converted to bilirubin by biliverdin reductase (31). HO-1 is an inducible form of HO that has emerged recently as a particularly attractive tool for the prevention and management of a broad range of human and animal diseases characterized by elevated levels of reactive oxygen-containing molecules (9). The expression of HO-1 is up-regulated in response to cellular stress and by several factors such as pro-oxidative stimuli, UV light, LPS, hydrogen peroxide, heat shock, and heavy metals (31). As an anti-inflammatory and immunosuppressive protein, HO-1 exerts immunomodulatory effects mainly through modulating T cell responses as well as influencing Tregs and probably inhibiting antigen-presenting cells (31). In recent years pharmacological or genetic up-regulation of HO-1 has been found to ameliorate disease symptoms in several autoimmune disorders, including lupus, rheumatoid arthritis, and experimental autoimmune encephalomyelitis (11, 32, 33). In a previous study our data showed that hemin, a major substrate of HO-1, could induce its expression and increase its activity (16) and plays a protective role in the eosinophilic asthma animal model. These observations coincide with those from other laboratories using guinea pig or rat models (34, 35). In this study our results further indicate that HO-1 is capable of inhibiting OVA-induced neutrophilic airway inflammation in a NEA mouse model using DO11.10 T-cell receptor transgenic mice. Moreover, transfection of HO-1 siRNA *in vivo* reduced hemin-induced HO-1 expression in DO11.10 mice, consistent with our previous observation in a neonatal hyperbilirubinemia rat model (21). The data indicated that knockdown of HO-1 by siRNA abolished the effect of hemin, leading to the aggravation of airway inflammation. It has been reported previously that inflammation in OVA-challenged DO11.10 or OTII mice is characterized by an increase in neutrophils instead of eosinophils without elevation in serum IgE, similar to NEA, and is mediated by Th17 responses. Therefore, this is generally considered to be a useful model for the investigation of antigen-induced Th17-mediated neutrophilic airway inflammation (22, 23, 36, 37). In the current study, we observed that OVA challenge resulted in an increased number of macrophages in BALF, consistent with findings reported by Nakagome *et al.* (37) and Tae *et al.* (38). The results indicate that the increased neutrophil response in mice with OVA-induced airway inflammation is accompanied by an increased number of macrophages. Meanwhile, our results showed that OVA challenge induced predominant Th17 responses rather than Th1 or Th2 responses in DO11.10 mice, which were suppressed by HO-1 induction, revealing an anti-inflammatory role for HO-1 in Th17-mediated immune responses.

Several investigations have demonstrated the potential role of HO-1 in the differentiation of various cells, such as osteoblasts (39), adipocytes (40), dendritic cells (41), and Kupffer cells (42), but it is still unclear whether HO-1 can directly affect Th17 cell differentiation. Thus, we supposed that the beneficial

FIGURE 7. **HO-1 does not noticeably affect Th1- or Th2-mediated response in DO11.10 mice.** *A*, ELISA analysis of IFN-γ in BALF obtained from four groups. *CON*, control. *B*, ELISA analysis of IL-4 in BALF collected from four groups. *C*, flow cytometric analysis of mediastinal lymph node (*LN*) and spleen (*SP*) cells isolated from DO11.10 mice in control, OVA, OVA + hemin, and OVA + SnPP groups. *Numbers in the upper left and lower right quadrants* indicate the percentages of Th1 ($CD4^+$IFN-γ^+) cells and Th2 ($CD4^+$IL-4^+) cells gated on $CD4^+$ T cells, respectively. Each symbol in the graph represents an individual mouse ($n = 6$). *D*, real-time PCR analysis of T-bet mRNAs in lung tissues from four groups. *E*, real-time PCR analysis of GATA-binding protein 3 mRNAs in lung tissues from four groups.

effect of HO-1 observed in our mouse model may be attributed to its inhibitory effect on Th17 cell differentiation. To validate this hypothesis, we conducted an *in vitro* study by utilizing purified naïve T cells from normal BALB/c mice and culturing them under Th17-skewing conditions. The results confirmed our speculation, showing that the proportion of Th17 cells declined in the presence of hemin. However, the proportion of Th17 cells was not noticeably affected by SnPP, indicating that the enzymatic activity of HO-1 is indispensable in its inhibitory effect. Moreover, hemin can mildly suppress the proliferation of $CD4^+$ T cells, which may be attributed to the anti-proliferative effect of CO (an enzymatic product of HO-1) on $CD4^+$ T cells via inhibition of IL-2 secretion (43) and caspase-8 expression (44). Therefore, our findings demonstrate a somewhat broader contribution of HO-1 to T cell differentiation.

Recently, imbalances in the development and function of Th17 cells and Tregs have been demonstrated to play an important role in autoimmune diseases. The Th17/Treg balance is considered to be critical for host immunity and the preservation of tolerance (45, 46). In addition, it has been proved that Th17 cells and Tregs can be interconverted and are reciprocally regulated during differentiation dependent on the cytokine milieu (47, 48). Tregs are responsible for maintaining immune homeostasis. They can suppress airway inflammation and improve airway remodeling by restraining excessive T-cell immunity, regulating the balance among Th subsets, and decreasing the production of proinflammatory cytokines (49, 50). The phosphorylation of STAT5 is considered critical for both Treg development and maintenance as well as Foxp3 expression (29) and is crucial for constraining Th17 cell development (51). Th17 cells, as a separate T cell subset involved in the pathophysiology of inflammatory diseases, require specific cytokines and transcription factors for their differentiation in which IL-6 and TGF-β are recognized as crucial factors (26, 45). During the process of Th17 cell differentiation, a signal transducer and activator of STAT3 and its downstream signaling molecule RORγt are the signature transcription factors (27, 52). STAT3 is known to be a primary factor in the downstream signaling of IL-6, the phosphorylation of which induces proinflammatory gene expression (53, 54). Furthermore, Treg cell differentiation can be suppressed by IL-6 via inhibition of the expression of Foxp3 in a STAT3-dependent fashion and thereby contribute to immune pathology (29, 55). Thus, it is believed that STAT3 is a key signaling molecule modulating the balance of Th17 cells and Tregs. Moreover, it has been reported that the interaction between HO-1 and STAT3 abrogates STAT3 activation, so that induction of HO-1 represses androgen receptor activity and affects prostate cancer cell tumorigenicity (56), suggesting that HO-1 can interfere with STAT3 signaling. Therefore, we assessed IL-6-induced phosphorylation of STAT3 in $CD4^+$ T cells from DO11.10 mice treated with or without hemin/SnPP to further study the underlying mechanisms of HO-1-regulated Th17/Treg balance. Interestingly, induction of HO-1 by hemin indeed decreased the protein level of p-STAT3 in $CD4^+$ T cells. It may be possible that the inhibition of RORγt expression and decrease of Th17 cell proportion in this animal model may be partly due to reduced phosphorylation of STAT3 as a result of HO-1 induction. However, we observed that HO-1 did not have an obvious effect on phosphorylation of STAT5. As there is a dynamic balance between the development of Th17 cells and Tregs (57), we consider that changes in the proportions of Tregs and production of IL-10 in our current study may be caused by suppressing RORγt and enhancing Foxp3. However, further analyses are needed to link the beneficial effect of HO-1 on asthma to an effect on key transcription factors of signaling events that underlie fate decisions of $CD4^+$ T cells toward distinct Th subsets. Moreover, some researchers have indicated that besides its products, HO-1 protein itself is involved in cellular signaling and regulation of gene transcription (58, 59), suggesting that nuclear transfer of HO-1 protein may contribute to its influence on gene expression. This is a novel point of view under which to investigate the anti-inflammatory mechanisms of HO-1 in our future work.

In summary, the present study indicates that induction of HO-1 suppresses Th17 response accompanied by up-regulation of Tregs in an OVA-induced non-eosinophilic asthma model. More importantly, TGF-β plus IL-6-induced Th17 cell differentiation *in vitro* is likely inhibited by HO-1 induction via down-regulation of p-STAT3. These data suggest that the inhibitory effect of HO-1 on Th17-mediated inflammation may be useful for developing novel therapeutic approaches in managing steroid-resistant asthma and other autoimmune diseases.

Acknowledgment—We thank the flow cytometry core facility at Shanghai Jiaotong University School of Medicine for flow cytometric analysis.

REFERENCES

1. Douwes, J., Gibson, P., Pekkanen, J., and Pearce, N. (2002) Non-eosinophilic asthma. Importance and possible mechanisms. *Thorax* **57,** 643–648
2. Simpson, J. L., Scott, R., Boyle, M. J., and Gibson, P. G. (2006) Inflammatory subtypes in asthma. Assessment and identification using induced sputum. *Respirology* **11,** 54–61
3. Kikuchi, S., Nagata, M., Kikuchi, I., Hagiwara, K., and Kanazawa, M. (2005) Association between neutrophilic and eosinophilic inflammation in patients with severe persistent asthma. *Int. Arch. Allergy Immunol.* **137,** 7–11
4. The ENFUMOSA Study Group (2003) The ENFUMOSA cross-sectional European multicentre study of the clinical phenotype of chronic severe asthma. *Eur. Respir. J.* **22,** 470–477
5. Oboki, K., Ohno, T., Saito, H., and Nakae, S. (2008) Th17 and allergy. *Allergol Int.* **57,** 121–134
6. Ouyang, W., Kolls, J. K., and Zheng, Y. (2008) The biological functions of T helper 17 cell effector cytokines in inflammation. *Immunity* **28,** 454–467
7. Wong, C. K., Lun, S. W., Ko, F. W., Wong, P. T., Hu, S. Q., Chan, I. H., Hui, D. S., and Lam, C. W. (2009) Activation of peripheral Th17 lymphocytes in patients with asthma. *Immunol. Invest.* **38,** 652–664
8. McKinley, L., Alcorn, J. F., Peterson, A., Dupont, R. B., Kapadia, S., Logar, A., Henry, A., Irvin, C. G., Piganelli, J. D., Ray, A., and Kolls, J. K. (2008) TH17 cells mediate steroid-resistant airway inflammation and airway hyperresponsiveness in mice. *J. Immunol.* **181,** 4089–4097
9. Haines, D. D., Lekli, I., Teissier, P., Bak, I., and Tosaki, A. (2012) Role of haeme oxygenase-1 in resolution of oxidative stress-related pathologies. Focus on cardiovascular, lung, neurological, and kidney disorders. *Acta physiologica* **204,** 487–501
10. Varga, C., Laszlo, F., Fritz, P., Cavicchi, M., Lamarque, D., Horvath, K., Posa, A., Berko, A., and Whittle, B. J. (2007) Modulation by heme and zinc protoporphyrin of colonic heme oxygenase-1 and experimental inflam-

matory bowel disease in the rat. *Eur. J. Pharmacol.* **561,** 164–171
11. Chora, A. A., Fontoura, P., Cunha, A., Pais, T. F., Cardoso, S., Ho, P. P., Lee, L. Y., Sobel, R. A., Steinman, L., and Soares, M. P. (2007) Heme oxygenase-1 and carbon monoxide suppress autoimmune neuroinflammation. *J. Clin. Invest.* **117,** 438–447
12. Zhong, W., Xia, Z., Hinrichs, D., Rosenbaum, J. T., Wegmann, K. W., Meyrowitz, J., and Zhang, Z. (2010) Hemin exerts multiple protective mechanisms and attenuates dextran sulfate sodium-induced colitis. *J. Pediatr Gastroenterol. Nutr.* **50,** 132–139
13. Yoriki, H., Naito, Y., Takagi, T., Mizusima, K., Hirai, Y., Harusato, A., Yamada, S., Tsuji, T., Kugai, M., Fukui, A., Higashimura, Y., Katada, K., Kamada, K., Uchiyama, K., Handa, O., Yagi, N., Ichikawa, H., and Yosikawa, T. (2013) Hemin ameliorates indomethacin-induced small intestinal injury in mice through the induction of heme oxygenase-1. *J. Gastroenterol. Hepatol.* **28,** 632–638
14. Correa-Costa, M., Semedo, P., Monteiro, A. P., Silva, R. C., Pereira, R. L., Gonçalves, G. M., Marques, G. D., Cenedeze, M. A., Faleiros, A. C., Keller, A. C., Shimizu, M. H., Seguro, A. C., Reis, M. A., Pacheco-Silva, A., and Câmara, N. O. (2010) Induction of heme oxygenase-1 can halt and even reverse renal tubule-interstitial fibrosis. *PLoS ONE* **5,** e14298
15. Hualin, C., Wenli, X., Dapeng, L., Xijing, L., Xiuhua, P., and Qingfeng, P. (2012) The anti-inflammatory mechanism of heme oxygenase-1 induced by hemin in primary rat alveolar macrophages. *Inflammation* **35,** 1087–1093
16. Xia, Z. W., Zhong, W. W., Xu, L. Q., Sun, J. L., Shen, Q. X., Wang, J. G., Shao, J., Li, Y. Z., and Yu, S. C. (2006) Heme oxygenase-1-mediated $CD4^+$CD25high regulatory T cells suppress allergic airway inflammation. *J. Immunol.* **177,** 5936–5945
17. Xia, Z. W., Xu, L. Q., Zhong, W. W., Wei, J. J., Li, N. L., Shao, J., Li, Y. Z., Yu, S. C., and Zhang, Z. L. (2007) Heme oxygenase-1 attenuates ovalbumin-induced airway inflammation by up-regulation of foxp3 T-regulatory cells, interleukin-10, and membrane-bound transforming growth factor-1. *Am. J. Pathol.* **171,** 1904–1914
18. Almolki, A., Guenegou, A., Golda, S., Boyer, L., Benallaoua, M., Amara, N., Bachoual, R., Martin, C., Rannou, F., Lanone, S., Dulak, J., Burgel, P. R., El-Benna, J., Leynaert, B., Leynaert, A. B., Aubier, M., and Boczkowski, J. (2008) Heme oxygenase-1 prevents airway mucus hypersecretion induced by cigarette smoke in rodents and humans. *Am. J. Pathol.* **173,** 981–992
19. Chang, T., Wu, L., and Wang, R. (2008) Inhibition of vascular smooth muscle cell proliferation by chronic hemin treatment. *Am. J. Physiol. Heart Circ. Physiol.* **295,** H999–H1007
20. Desbuards, N., Rochefort, G. Y., Schlecht, D., Machet, M. C., Halimi, J. M., Eder, V., Hyvelin, J. M., and Antier, D. (2007) Heme oxygenase-1 inducer hemin prevents vascular thrombosis. *Thromb. Haemost* **98,** 614–620
21. Wu, J., Su, W., Jin, Y., Shi, Y., Li, C., Zhong, W., Zhang, X., Zhang, Z., and Xia, Z. (2009) Targeted suppression of heme oxygenase-1 by small interference RNAs inhibits the production of bilirubin in neonatal rat with hyperbilirubinemia. *BMC Mol. Biol.* **10,** 77
22. Knott, P. G., Gater, P. R., and Bertrand, C. P. (2000) Airway inflammation driven by antigen-specific resident lung $CD4^+$ T cells in $\alpha\beta$-T cell receptor transgenic mice. *Am. J. Respir. Crit. Care Med.* **161,** 1340–1348
23. Wilder, J. A., Collie, D. D., Bice, D. E., Tesfaigzi, Y., Lyons, C. R., and Lipscomb, M. F. (2001) Ovalbumin aerosols induce airway hyperreactivity in naive DO11.10 T cell receptor transgenic mice without pulmonary eosinophilia or OVA-specific antibody. *J. Leukoc. Biol.* **69,** 538–547
24. Tanaka, S., Yoshimoto, T., Naka, T., Nakae, S., Iwakura, Y., Cua, D., and Kubo, M. (2009) Natural occurring IL-17 producing T cells regulate the initial phase of neutrophil mediated airway responses. *J. Immunol.* **183,** 7523–7530
25. Durant, L., Watford, W. T., Ramos, H. L., Laurence, A., Vahedi, G., Wei, L., Takahashi, H., Sun, H. W., Kanno, Y., Powrie, F., and O'Shea, J. J. (2010) Diverse targets of the transcription factor STAT3 contribute to T cell pathogenicity and homeostasis. *Immunity* **32,** 605–615
26. Kimura, A., and Kishimoto, T. (2010) IL-6. Regulator of Treg/Th17 balance. *Eur. J. Immunol.* **40,** 1830–1835
27. Yang, X. P., Ghoreschi, K., Steward-Tharp, S. M., Rodriguez-Canales, J., Zhu, J., Grainger, J. R., Hirahara, K., Sun, H. W., Wei, L., Vahedi, G., Kanno, Y., O'Shea, J. J., and Laurence, A. (2011) Opposing regulation of the locus encoding IL-17 through direct, reciprocal actions of STAT3 and STAT5. *Nat. Immunol.* **12,** 247–254
28. Fontenot, J. D., Gavin, M. A., and Rudensky, A. Y. (2003) Foxp3 programs the development and function of $CD4^+CD25^+$ regulatory T cells. *Nat. Immunol.* **4,** 330–336
29. Yao, Z., Kanno, Y., Kerenyi, M., Stephens, G., Durant, L., Watford, W. T., Laurence, A., Robinson, G. W., Shevach, E. M., Moriggl, R., Hennighausen, L., Wu, C., and O'Shea, J. J. (2007) Nonredundant roles for Stat5a/b in directly regulating Foxp3. *Blood* **109,** 4368–4375
30. Zijlstra, G. J., Ten Hacken, N. H., Hoffmann, R. F., van Oosterhout, A. J., and Heijink, I. H. (2012) Interleukin-17A induces glucocorticoid insensitivity in human bronchial epithelial cells. *Eur. Respir J.* **39,** 439–445
31. Grochot-Przeczek, A., Dulak, J., and Jozkowicz, A. (2012) Haem oxygenase-1. Non-canonical roles in physiology and pathology. *Clin. Sci.* **122,** 93–103
32. Takeda, Y., Takeno, M., Iwasaki, M., Kobayashi, H., Kirino, Y., Ueda, A., Nagahama, K., Aoki, I., and Ishigatsubo, Y. (2004) Chemical induction of HO-1 suppresses lupus nephritis by reducing local iNOS expression and synthesis of anti-dsDNA antibody. *Clin. Exp. Immunol.* **138,** 237–244
33. Kobayashi, H., Takeno, M., Saito, T., Takeda, Y., Kirino, Y., Noyori, K., Hayashi, T., Ueda, A., and Ishigatsubo, Y. (2006) Regulatory role of heme oxygenase 1 in inflammation of rheumatoid arthritis. *Arthritis Rheum.* **54,** 1132–1142
34. Almolki, A., Taillé, C., Martin, G. F., Jose, P. J., Zedda, C., Conti, M., Megret, J., Henin, D., Aubier, M., and Boczkowski, J. (2004) Heme oxygenase attenuates allergen-induced airway inflammation and hyperreactivity in guinea pigs. *Am. J. Physiol. Lung Cell. Mol. Physiol.* **287,** L26–L34
35. Jia, Y. X., Sekizawa, K., Okinaga, S., Lie, R., and Sasaki, H. (1999) Role of heme oxygenase in pulmonary response to antigen challenge in sensitized rats *in vivo*. *Int. Arch. Allergy Immunol.* **120,** 141–145
36. Nakae, S., Suto, H., Berry, G. J., and Galli, S. J. (2007) Mast cell-derived TNF can promote Th17 cell-dependent neutrophil recruitment in ovalbumin-challenged OTII mice. *Blood* **109,** 3640–3648
37. Nakagome, K., Imamura, M., Okada, H., Kawahata, K., Inoue, T., Hashimoto, K., Harada, H., Higashi, T., Takagi, R., Nakano, K., Hagiwara, K., Kanazawa, M., Dohi, M., Nagata, M., and Matsushita, S. (2011) Dopamine D1-like receptor antagonist attenuates Th17-mediated immune response and ovalbumin antigen-induced neutrophilic airway inflammation. *J. Immunol.* **186,** 5975–5982
38. Tae, Y. M., Park, H. T., Moon, H. G., Kim, Y. S., Jeon, S. G., Roh, T. Y., Bae, Y. S., Gho, Y. S., Ryu, S. H., Kwon, H. S., and Kim, Y. K. (2012) Airway activation of formyl peptide receptors inhibits Th1 and Th17 cell responses via inhibition of mediator release from immune and inflammatory cells and maturation of dendritic cells. *J. Immunol.* **188,** 1799–1808
39. Lin, T. H., Tang, C. H., Hung, S. Y., Liu, S. H., Lin, Y. M., Fu, W. M., and Yang, R. S. (2010) Upregulation of heme oxygenase-1 inhibits the maturation and mineralization of osteoblasts. *J. Cell Physiol.* **222,** 757–768
40. Vanella, L., Kim, D. H., Asprinio, D., Peterson, S. J., Barbagallo, I., Vanella, A., Goldstein, D., Ikehara, S., Kappas, A., and Abraham, N. G. (2010) HO-1 expression increases mesenchymal stem cell-derived osteoblasts but decreases adipocyte lineage. *Bone* **46,** 236–243
41. Chauveau, C., Rémy, S., Royer, P. J., Hill, M., Tanguy-Royer, S., Hubert, F. X., Tesson, L., Brion, R., Beriou, G., Gregoire, M., Josien, R., Cuturi, M. C., and Anegon, I. (2005) Heme oxygenase-1 expression inhibits dendritic cell maturation and proinflammatory function but conserves IL-10 expression. *Blood* **106,** 1694–1702
42. Devey, L., Ferenbach, D., Mohr, E., Sangster, K., Bellamy, C. O., Hughes, J., and Wigmore, S. J. (2009) Tissue-resident macrophages protect the liver from ischemia reperfusion injury via a heme oxygenase-1-dependent mechanism. *Mol. Ther.* **17,** 65–72
43. Pae, H. O., Oh, G. S., Choi, B. M., Chae, S. C., Kim, Y. M., Chung, K. R., and Chung, H. T. (2004) Carbon monoxide produced by heme oxygenase-1 suppresses T cell proliferation via inhibition of IL-2 production. *J. Immunol.* **172,** 4744–4751
44. Song, R., Mahidhara, R. S., Zhou, Z., Hoffman, R. A., Seol, D. W., Flavell, R. A., Billiar, T. R., Otterbein, L. E., and Choi, A. M. (2004) Carbon monoxide inhibits T lymphocyte proliferation via caspase-dependent pathway. *J. Immunol.* **172,** 1220–1226

45. Bettelli, E., Carrier, Y., Gao, W., Korn, T., Strom, T. B., Oukka, M., Weiner, H. L., and Kuchroo, V. K. (2006) Reciprocal developmental pathways for the generation of pathogenic effector TH17 and regulatory T cells. *Nature* **441,** 235–238
46. Bettelli, E., Korn, T., Oukka, M., and Kuchroo, V. K. (2008) Induction and effector functions of T(H)17 cells. *Nature* **453,** 1051–1057
47. Ye, J., Su, X., Hsueh, E. C., Zhang, Y., Koenig, J. M., Hoft, D. F., and Peng, G. (2011) Human tumor-infiltrating Th17 cells have the capacity to differentiate into IFN-γ^+ and Foxp3$^+$ T cells with potent suppressive function. *Eur. J. Immunol.* **41,** 936–951
48. Lee, Y. K., Mukasa, R., Hatton, R. D., and Weaver, C. T. (2009) Developmental plasticity of Th17 and Treg cells. *Curr. Opin. Immunol.* **21,** 274–280
49. Robinson, D. S. (2009) Regulatory T cells and asthma. *Clin. Exp. Allergy* **39,** 1314–1323
50. Presser, K., Schwinge, D., Wegmann, M., Huber, S., Schmitt, S., Quaas, A., Maxeiner, J. H., Finotto, S., Lohse, A. W., Blessing, M., and Schramm, C. (2008) Coexpression of TGF-beta1 and IL-10 enables regulatory T cells to completely suppress airway hyperreactivity. *J. Immunol.* **181,** 7751–7758
51. Laurence, A., Tato, C. M., Davidson, T. S., Kanno, Y., Chen, Z., Yao, Z., Blank, R. B., Meylan, F., Siegel, R., Hennighausen, L., Shevach, E. M., and O'shea, J. J. (2007) Interleukin-2 signaling via STAT5 constrains T helper 17 cell generation. *Immunity* **26,** 371–381
52. Ivanov, I. I., McKenzie, B. S., Zhou, L., Tadokoro, C. E., Lepelley, A., Lafaille, J. J., Cua, D. J., and Littman, D. R. (2006) The orphan nuclear receptor RORγt directs the differentiation program of proinflammatory IL-17+ T helper cells. *Cell* **126,** 1121–1133
53. Gao, H., and Ward, P. A. (2007) STAT3 and suppressor of cytokine signaling 3. Potential targets in lung inflammatory responses. *Expert Opin. Ther. Targets* **11,** 869–880
54. Scott, M. J., Godshall, C. J., and Cheadle, W. G. (2002) Jaks, STATs, cytokines, and sepsis. *Clin. Diagn Lab. Immunol.* **9,** 1153–1159
55. Korn, T., Mitsdoerffer, M., Croxford, A. L., Awasthi, A., Dardalhon, V. A., Galileos, G., Vollmar, P., Stritesky, G. L., Kaplan, M. H., Waisman, A., Kuchroo, V. K., and Oukka, M. (2008) IL-6 controls Th17 immunity *in vivo* by inhibiting the conversion of conventional T cells into Foxp3$^+$ regulatory T cells. *Proc. Natl. Acad. Sci. U.S.A.* **105,** 18460–18465
56. Elguero, B., Gueron, G., Giudice, J., Toscani, M. A., De Luca, P., Zalazar, F., Coluccio-Leskow, F., Meiss, R., Navone, N., De Siervi, A., and Vazquez, E. (2012) Unveiling the association of STAT3 and HO-1 in prostate cancer. Role beyond heme degradation. *Neoplasia* **14,** 1043–1056
57. Muranski, P., and Restifo, N. P. (2013) Essentials of Th17 cell commitment and plasticity. *Blood* **121,** 2402–2414
58. Hori, R., Kashiba, M., Toma, T., Yachie, A., Goda, N., Makino, N., Soejima, A., Nagasawa, T., Nakabayashi, K., and Suematsu, M. (2002) Gene transfection of H25A mutant heme oxygenase-1 protects cells against hydroperoxide-induced cytotoxicity. *J. Biol. Chem.* **277,** 10712–10718
59. Lin, Q., Weis, S., Yang, G., Weng, Y. H., Helston, R., Rish, K., Smith, A., Bordner, J., Polte, T., Gaunitz, F., and Dennery, P. A. (2007) Heme oxygenase-1 protein localizes to the nucleus and activates transcription factors important in oxidative stress. *J. Biol. Chem.* **282,** 20621–20633